International Research Journal of Engineering and Technology (IRJET) e-ISSN: 2395-0056
Volume: 11 Issue: 08 | Aug 2024 www.irjet.net p-ISSN: 2395-0072

Experimental and FEM Analysis (ANSYS) of Conventional and BFRP Composite Beam

[1]Sourabh M. Kadam, [2]Dr.Chetan Patil

[1]Student Sanjay Ghodawat University Kolhapur, India.
[2]Profesor, Sanjay Ghodawat University Kolhapur, India.

Abstract - *This study investigates the mechanical behavior and structural performance of conventional and BERP (Basalt Fiber Reinforced Polymer) composite beams through both experimental testing and Finite Element Method (FEM) analysis using ANSYS software. The primary objective is to evaluate and compare the performance characteristics of these beams under various loading conditions to determine their suitability for advanced structural applications. Experimental tests were conducted to gather empirical data on stress, strain, and deflection for both types of beams. Concurrently, FEM analysis in ANSYS was employed to simulate these conditions, enabling a comprehensive assessment of stress distribution, deformation patterns, and potential failure points. The results indicate a strong correlation between the experimental data and FEM simulations, affirming the reliability of the computational models. The BERP composite beams exhibited enhanced performance metrics, including higher strength, improved durability, and superior resistance to environmental factors, compared to their conventional counterparts. These findings suggest that BERP composite beams offer a promising alternative for applications demanding high-performance materials with extended service life and reduced maintenance requirements*

Key Words: Basalt Fiber Reinforced Polymer sheets, wrapping, mechanical properties, Flexural Strength, durability

1.INTRODUCTION

Recently, there has been a significant increase in the focus on developing infrastructure constructed using concrete. Concrete structures, however, face a variety of issues over time, including degradation, increased load demands due to new design codes, overloading, poor or insufficient design of existing structures, lack of quality control, and changes in the use of these structures. The rapid deterioration of concrete is a serious challenge for engineers, not only on this continent but globally. It is imperative to address structures displaying signs of degradation or damage promptly. If these issues are not treated in a timely manner, the structures risk becoming unsafe and unusable. Strengthening or repairing older structures is essential to maintain their efficient serviceability and to fulfil the demands of newer constructions. Compared to the alternative of rebuilding, repairing or strengthening existing structures is advantageous both economically and environmentally.

There is often a correlation between the deterioration of infrastructure and the need to meet stricter design criteria. This has led to a substantial increase in attention worldwide towards revitalizing infrastructure that results from civil engineering. Strengthening and upgrading structures that are structurally deficient or defective is both a technically sound and practical method. In addition to determining the strength of the material, it is necessary to investigate the origin of the damage and predict its future performance. Assessing the remaining life of these structures is of utmost importance. Identifying the cause of deterioration and conducting an accurate assessment of the structural integrity of the structures can make repairing these structures financially viable and extend their lifespan.

Members that have suffered significant damage should have their current status evaluated promptly. To determine the future load-carrying capacity and behavioral capabilities of the structural elements, various parameters must be considered once the members at risk of significant damage are identified. To ensure a thorough post-repair evaluation, appropriate tests utilizing non-destructive testing methods can be conducted. Under these circumstances, employing a scientific and systematic procedure to evaluate the properties of damaged structures is of the utmost importance. This approach ensures that the evaluation is accurate and reliable, providing crucial information to guide the repair and strengthening process.

In summary, the challenges posed by the deterioration of concrete structures require immediate attention and a systematic approach to evaluation and repair. By addressing these issues promptly and effectively, engineers can extend the lifespan of existing structures, ensuring their safety and functionality while meeting the demands of modern design codes. This approach not only enhances the sustainability of infrastructure but also provides significant economic and environmental benefits.

.

1.1 NEED OF THE STUDY

Basalt fibers are formed by melting and mixing natural basalt rock with other primal materials. This produces various types of basalt fibers with distinct properties, such as high strength, resistance to chemicals and heat, and low density. Basalt fibers are versatile materials with a unique combination of properties. Although basalt fibers offer high strength, low density, and an economical price. Many old constructions require repair to prevent minor cracks from leading to structural failure over time. Basalt Fiber Sheets offer a solution for advanced repair to extend the lifespan of buildings. Various wrapping techniques can be selected based on crack patterns to increase the life span of buildings

2. METHODOLOGY AND MATERIAL

Following Figure No. 1 shows the methodology adopted for the proposed work.

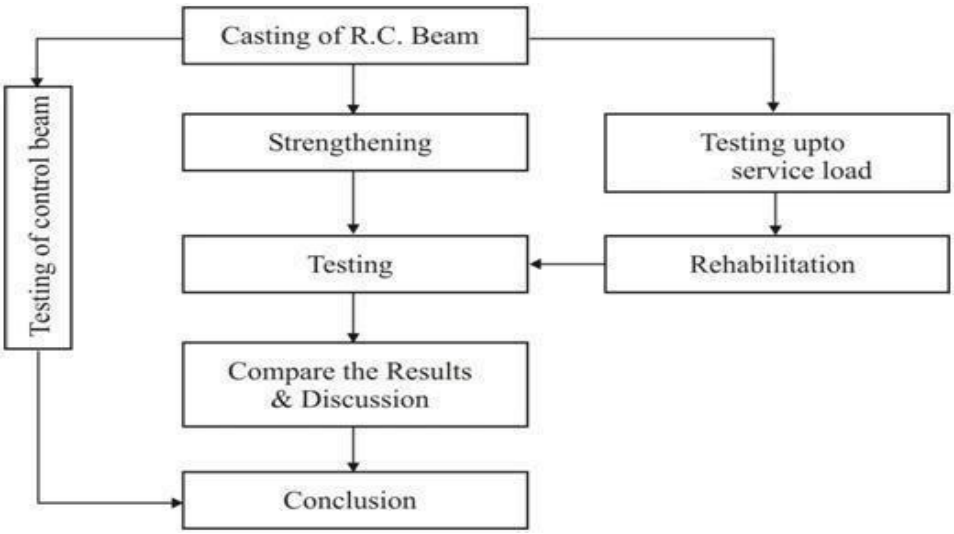

Figure 1 Methodology of Project work

A. Test Specimens

The strength property of concrete are determined by casting specimens of cube size 150 mm×150 mm ×150 mm compression, beam of size 700 mm× 100 mm× 200 mm for flexure strength and cured 28 days

B. Materials

M20 Grade Concrete Mix Design

The design of a concrete mix for M20 grade follows guidelines provided by IS 456:2000 and IS 10262:2019. Here's a step-by-step approach:

Water-Cement Ratio:

For M20 grade concrete, a water-cement (w/c) ratio of 0.45 is commonly used. This ratio is selected based on experience and the requirement for achieving the desired workability and strength.

Water Content:

According to Table 2 of IS 10262:2019, the approximate water content for a maximum aggregate size of 20 mm is 186 kg for a slump range of 25-50 mm. Adjustments to this value may be needed based on specific project requirements.

Cement Content:

The minimum cement content for durability, as per IS 456:2000, is 320 kg/m^3. Verify that the calculated cement content meets this minimum requirement.

Proportion of Coarse Aggregate:

Based on IS 10262:2019, for a w/c ratio of 0.50, the volume proportion of coarse aggregate (by mass) is approximately 0.62. This proportion should be adjusted based on the actual w/c ratio used in the mix design.

Calculation of Aggregates:

Compute the mass of aggregates by multiplying the volume of each aggregate by its specific gravity. Convert these volumes to mass to determine the correct amount of each aggregate to use.

Mix Proportions:

The final mix proportions for M20 grade concrete are determined as follows:

Table 1 Final mix of M30 grade concrete by using IS 10262:2019 (kg/m3)

Cementous Material		Fine Aggregate	Coarse Aggregate		Water	Admixture
Cement	Fly Ash		10 mm	20 mm		
280	40	696	100	1029	145	2.85
320		696	1129		145	
1.00		2.18	3.53		0.45	

The compressive strength of concrete is a key property that is assessed as per Indian Standards (IS). The specific code governing the compressive strength of concrete is IS 516:1959, The standard test method for determining the compressive strength of concrete involves testing a cube specimen of size 150 mm x 150 mm x 150 mm. The specimen is subjected to a compressive force until failure. The compressive strength is calculated as the load applied at the point of failure divided by the cross-sectional area of the specimen. Concrete cubes are cast and cured for a specific period, typically 28 days. The machine should apply the load uniformly without shock and increase continuously at a specified rate until the specimen fails. The load is applied at a rate of 140 kg/cm^2 per minute.

Table 2 The compressive strength of concrete of final concrete mix.

Sr. No.	Age (days)	Weight (kg)	Crushing Load (kN)	Compressive Strength (N/mm^2)	Avg Compressive Strength (N/mm^2)
1	7	8.84	405	18.00	17.48
2		8.87	380	16.89	
3		8.94	395	17.56	
4	28	8.91	540	24.00	24.52
5		8.88	560	24.89	
6		8.96	555	24.67	

Design of RC Beam as per IS 456 -2000

To calculate the center point load carrying capacity of a simply supported reinforced concrete (RC) beam using the limit state method as per IS 456:2000.

Given data:

1) Main steel - 2#10 at bottom

2) Top steel - 2#10 at top

3) Stirrups - 6T @ 125mm

Properties of BFRP

Table -3: The properties of BFRP

Properties	Values
Tensile Strength (MPa)	3000
Modulus of Elasticity (GPa)	110
Nominal thick (mm)	0.3
Elongation %	2.6
Weight of the sheet per m2 (g/m2)	300

Properties Epoxy Resin

Table 4 : Properties of Epoxy Resin

Property	Epoxy Resin
Appearance	Clear low viscosity liquid
Viscosity at 30°C	550-650 cps
Type	Room temperature cure
Epoxy Equivalent	180 – 200
Specific Gravity at 30°C	1.1-1.2
Storage Stability	1 year

3.Testing of RC Beam Section for Three-Point Loading in UTM

Testing a reinforced concrete (RC) beam section under three-point loading involves placing the beam on a Universal Testing Machine (UTM) and applying a load at a single central point while supporting the beam at both ends. This test helps determine the load carrying capacity and behavior of the beam under load. The testing of a reinforced concrete (RC) beam under three-point loading is conducted using a Universal Testing Machine (UTM) with a capacity of 1200 kN. Here is a detailed procedure for conducting this test:

a) Beam Specimen Preparation:

Ensure the RC beam is prepared according to the specified dimensions and curing conditions. If retrofitting with BFRP, ensure the wrapping process is completed and the epoxy has cured properly.

b) Setting Up the UTM:

Place the beam on the supports of the UTM. The supports should be properly aligned and spaced to create the required span length for the test. Measure and set the span length between the supports, typically to a standard length such as 500 mm.

c) Test Procedure

Center the beam on the supports, ensuring it is aligned correctly with the loading apparatus. Attach any necessary measurement devices such as strain gauges or deflection sensors at the designated locations on the beam.

d) Applying the Load:

Gradually apply the load at a constant rate through the loading head. The load should be applied smoothly to avoid any sudden shocks. Continuously monitor the load and deflection readings. Use a digital indicator or dial gauge placed at the bottom center of the beam to measure deflection accurately.

e) Observing the Beam:

Crack Patterns: Observe and record the development of cracks on the beam as the load increases. Note the locations, orientations, and types of cracks (e.g., flexural or shear cracks). Continue applying the load until the beam reaches its maximum load capacity and fails. Record the maximum load (P) the beam can withstand before failure.

f) Recording Data:

Record the deflection readings at various load increments. Plot the load-deflection curve to analyze the behavior of the beam under load.

Figure 2 Testing of RC beam section for three-point loading in UTM

4.Result & Discussion

4.1 Load Carrying Capacity of RC Beams

The load-carrying capacity of reinforced concrete (RC) beams is a critical parameter in structural engineering, reflecting the beam's ability to withstand applied loads without failing. This capacity is determined through various testing and analytical methods, with the three-point loading test in a Universal Testing Machine (UTM).

Table 5 Load carrying capacity for RC Beams

Beam No	Load at First Crack (kN)	Deflection at First Crack (mm)	Load at Failure (kN)	Deflection at Failure (mm)	Elastic Load Carrying Capacity as per IS 456:2000 (kN)
B10	59.38	1.701	113.22	4.43	64.05
B11	60.12	1.736	94.74	3.300	64.05
B12	67.73	2.238	102.49	4.190	64.05

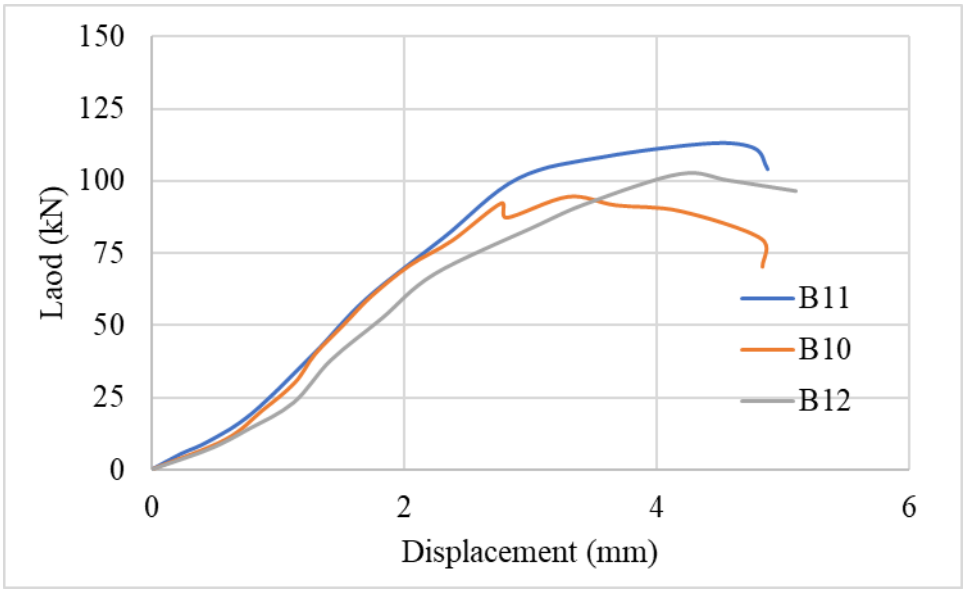

Figure 3 The load-displacement curves for three different beams

The Figure 3 shows the load-displacement curves for three different beams (B10, B11, and B12). All three beams show similar initial stiffness, as indicated by the steepness of the curves in the initial linear portion of the graph. Beam B12 exhibits slightly lower initial stiffness compared to B10 and B11, as its curve starts to deviate from the others at lower loads. The first visible deviation from linearity, which corresponds to the formation of the first crack, occurs at different load levels for each beam. Beam B12 reaches a noticeable crack at around 60-65 kN, while B10 and B11 show cracking behavior at slightly lower loads. Beam B10 has the highest ultimate load, peaking close to 113 kN before failure. Beam B11 reaches a slightly lower peak load compared to B10, around 95 kN. Beam B12 shows an ultimate load of about 102 kN, which is lower than B10 but higher than B11

c) Beam B12

Figure **Error! No text of specified style in document.** The crack development at ultimate load for RC beams

4.2 Pre-Cracking of RC Beams

Table 6 Load carrying capacity for RC Beams @ pre-cracking

Beam No	Load at First Crack (kN)	Deflection at First Crack (mm)	Crack Pattern Observation
B1	71.06	2.365	The cracks are narrow and vertical start from the bottom surface of the beam (tension face & bottom) and propagate upward towards the neutral axis.
B2	59.65	1.982	The cracks are narrow and vertical start from the bottom surface of the beam (tension face) and propagate upward towards the neutral axis.
B3	50.37	2.340	The cracks are narrow and vertical start from the bottom surface of the beam (tension face) and propagate upward towards the neutral axis.
B4	50.57	1.722	Thes cracks appear fine and straight, typically forming perpendicular to the beam's axis.
B5	54.11	2.179	Thes cracks appear fine and straight, typically forming perpendicular to the beam's axis.
B6	67.34	2.727	The cracks are narrow and vertical start from the bottom surface of the beam (tension face) and propagate upward towards the neutral axis.
B7	51.07	2.226	The cracks are narrow and vertical start from the bottom surface of the beam (tension face & bottom) and propagate upward towards the neutral axis.
B8	59.96	2.169	The cracks are narrow and vertical start from the bottom surface of the beam (tension face & bottom) and propagate upward towards the neutral axis.
B9	59.29	1.989	Thes cracks appear fine and straight, typically forming perpendicular to the beam's axis.

From Table 6, the load at which the first crack occurs varies among the beams, ranging from 50.37 kN to 71.06 kN. Beam B1 shows the highest load at the first crack (71.06 kN), indicating a higher initial stiffness and possibly better material properties or reinforcement configuration. Beam B3 has the lowest load at first crack (50.37 kN), suggesting that it may have the weakest performance in terms of initial load-carrying capacity among the tested beams.

The deflection at the first crack also varies, with values ranging from 1.722 mm to 2.727 mm. Beam B4 shows the smallest deflection at first crack (1.722 mm), indicating a stiffer response to loading up to the point of cracking. Beam B6 exhibits the largest deflection at first crack (2.727 mm), which suggests a more ductile response but may also indicate the potential for larger deflections under service loads.

Beams B1, B2, B3, B6, B7, and B8 exhibit narrow, vertical cracks that initiate at the bottom surface (tension face) and propagate upward towards the neutral axis. This crack pattern is typical of flexural failure and indicates that these beams are responding to the tensile stresses in the expected manner. Beams B4, B5, and B9 display fine and straight cracks, typically forming perpendicular to the beam's axis. These cracks suggest a more uniform stress distribution and may indicate a different cracking mechanism or a different stage of crack development.

The presence of narrow, vertical cracks is consistent with expected flexural behavior under loading, where tensile stresses cause cracking in the concrete. The fine, straight cracks observed in some beams may indicate a more gradual crack development or a different stress distribution within the beam. The deflections at first crack, particularly for beams like B6 with a deflection of 2.727 mm, indicate the importance of considering deflection limits in design to prevent excessive cracking and ensure long-term serviceability of the structure.

Table 7 Retrofitting of RC beams with BFRP

Beam No	Specimen Id.	Description
B1	B1U	Wrapped with a single layer of multidirectional BFRP fabric @ two sides and bottom face.
B2	B2S	Wrapped with a single layer of multidirectional BFRP fabric @ two sides only.
B3	B3S	Wrapped with a single layer of multidirectional BFRP fabric @ two sides only.
B4	B4B	Wrapped with a single layer of multidirectional BFRP fabric @ bottom face only.
B5	B5B	Wrapped with a single layer of multidirectional BFRP fabric @ bottom face only.
B6	B6S	Wrapped with a single layer of multidirectional BFRP fabric @ two sides only.
B7	B7U	Wrapped with a single layer of multidirectional BFRP fabric @ two sides and bottom face.
B8	B8U	Wrapped with a single layer of multidirectional BFRP fabric @ two sides and bottom face.
B9	B9B	Wrapped with a single layer of multidirectional BFRP fabric @ bottom face only.

4.3 The RC Beams with BFRP Fabric @ Two Sides and Bottom Face (BU).

A reinforced concrete (RC) beam with Basalt Fiber Reinforced Polymer (BFRP) fabric on two sides and the bottom face.

Figure.1 The RC Beam with BFRP fabric @ two sides and bottom face

Table 8 Load carrying capacity for RC Beams with BFRP fabric @ two sides and bottom face

Beam No	Load at Failure (kN)	Deflection at Failure (mm)	Average Load at Failure (kN)	Average Load at Failure for Control Beam (kN)	% Load increase
B1U	125.69	4.609	123.06	102.72	19.8
B7U	126.83	7.015			
B8U	116.67	6.204			

The experimental results for the RC beams retrofitted with Basalt Fiber Reinforced Polymer (BFRP) fabric reveal notable improvements in performance. The beams were tested to failure under controlled conditions, and the data collected includes the load at failure and deflection at failure for each beam. The results for the beams retrofitted with BFRP fabric, denoted as B1U, B7U, and B8U, are summarized in Table 6. The average load at failure for the BFRP-retrofitted beams is 123.06 kN, which is significantly higher compared to the control beam, which had an average failure load of 102.72 kN. The comparison shows that

the retrofitted beams exhibit a substantial increase in load-carrying capacity. The average increase in load-carrying capacity for the BFRP-retrofitted beams is approximately 19.8%. This enhancement indicates that the BFRP fabric is effective in increasing the structural strength of RC beams. While the load-carrying capacity has increased, there is a notable variation in deflection among the BFRP-retrofitted beams. The deflections at failure for the retrofitted beams ranged from 4.609 mm to 7.015 mm. This variability could be attributed to differences in the application of the BFRP fabric, surface preparation, or other experimental factors.

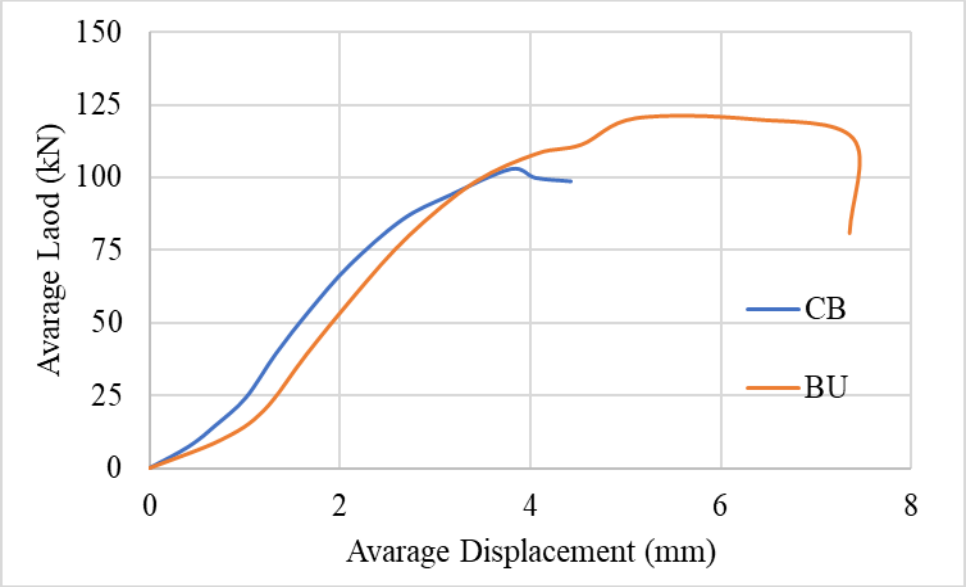

Figure 6 The load deflection curve for control beam (CB) & RC Beams with BFRP fabric @ two sides and bottom face (BU)

Figure 6 presents the load-deflection behavior of the control beam (CB) and an RC beam retrofitted with BFRP fabric on two sides and the bottom face (BU). The curves illustrate how both beams respond to increasing loads, providing insight into their stiffness, strength, and failure modes. In the initial loading phase, both beams exhibit a linear relationship between load and displacement, indicating elastic behavior. The slopes of the curves in this region suggest that the stiffness of the retrofitted beam (BU) is slightly higher than that of the control beam (CB). This suggests that the BFRP fabric enhances the beam's initial rigidity.

4.4 The RC Beams with BFRP Fabric @ Two Sides Face Only (BS).

A reinforced concrete (RC) beam with Basalt Fiber Reinforced Polymer (BFRP) fabric on two sides face

b) Beam B3
Figure 7 The RC Beam with BFRP fabric @ two sides face only

Table 10 Load carrying capacity for RC Beams with BFRP fabric @ two sides only (BS)

Beam No	Load at Failure (kN)	Deflection at Failure (mm)	Average Load at Failure (kN)	Average Load at Failure for Control Beam (kN)	% Load increase
B2S	111.55	4.942	105.58	102.72	2.79
B3S	101.98	4.554			
B6S	103.20	3.480			

The experimental results highlight the effect of BFRP retrofitting on the load-carrying capacity of RC beams. The average load at failure for the beams retrofitted with BFRP on two sides (BS) was found to be 105.58 kN. When compared to the control beam (CB), which had an average failure load of 102.72 kN, the retrofitted beams showed a modest improvement in load-carrying capacity, with a percentage increase of approximately 2.79%. This increase suggests that BFRP retrofitting on two sides enhances the structural capacity of the beam, although the improvement is relatively minor compared to other configurations, such as full U-wrapping. The modest gain may be due to the limited surface area covered by the BFRP fabric, which only partially supports the beam under flexural stress.

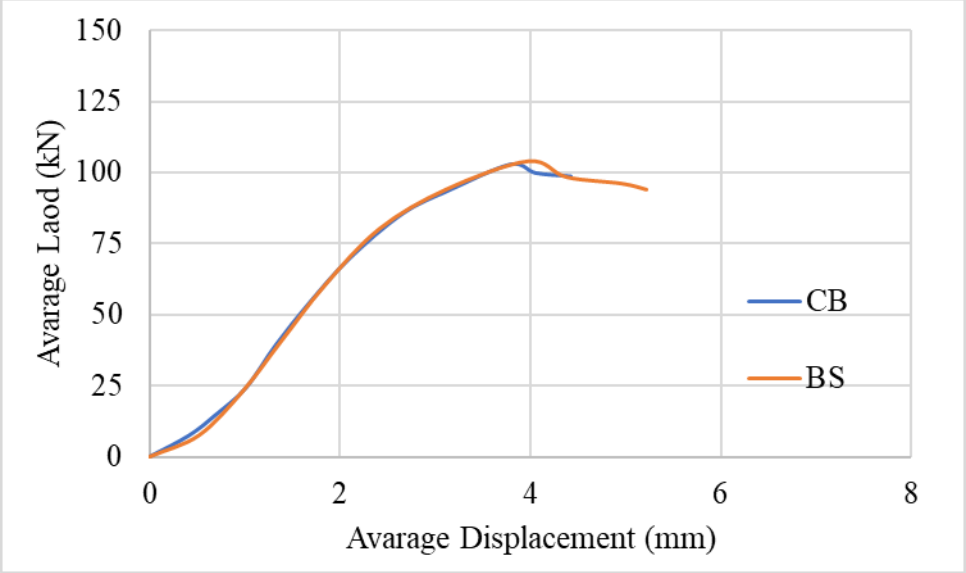

Figure 8 The load deflection curve for control beam (CB) & RC Beams with BFRP fabric @ two sides only (BS)

Figure 8 compares the load-deflection behavior of the control beam (CB) with that of an RC beam retrofitted with BFRP fabric on two sides only (BS). Both beams exhibit a linear load-deflection relationship in the initial phase, indicating elastic behavior. The similarity in the slopes of the two curves during this phase suggests that the BFRP fabric on the sides does not significantly alter the initial stiffness of the beam. As the load increases, both beams begin to exhibit nonlinear behavior, typically associated with the onset of cracking and other inelastic deformations. The retrofitted beam (BS) shows a slightly delayed transition into the nonlinear range compared to the control beam (CB), indicating that the side-applied BFRP fabric provides some additional resistance to initial cracking.

4.5 The RC Beams with BFRP Fabric @ Bottom Face Only (BB).

A reinforced concrete (RC) beam with Basalt Fiber Reinforced Polymer (BFRP) fabric on two sides face.

Figure 9 The RC Beam with BFRP fabric @ two sides face only

Table 11 Load carrying capacity for RC Beams with BFRP fabric @ bottom sides only (BB)

Beam No	Load at Failure (kN)	Deflection at Failure (mm)	Average Load at Failure (kN)	Average Load at Failure for Control Beam (kN)	% Load increase
B4B	100.53	4.798	120.90	102.72	17.70
B5B	135.23	6.449			
B9B	126.95	5.501			

The experimental analysis of the RC beams retrofitted with BFRP fabric on the bottom side only (BB) shows a notable improvement in their load-carrying capacity. The average load at failure for these retrofitted beams was found to be 120.90 kN. This is a significant enhancement compared to the control beam, which had an average load at failure of 102.72 kN. The application of BFRP on the bottom face alone led to a 17.7% increase in load-carrying capacity. This result highlights the effectiveness of BFRP retrofitting in strengthening RC beams, even when applied only to the bottom side. The increase in capacity can be attributed to the additional tensile reinforcement provided by the BFRP fabric, which effectively resists the tensile forces induced by bending.

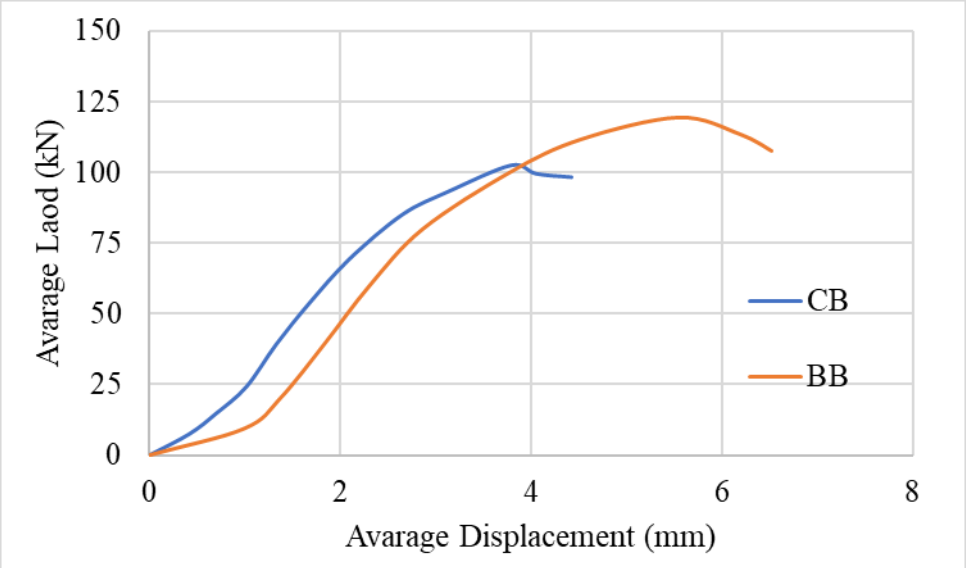

Figure 10 The load deflection curve for control beam (CB) & RC Beams with BFRP fabric @ bottom face (BB)

Figure 10 illustrates the load-deflection response of the control beam (CB) compared to an RC beam retrofitted with BFRP fabric on the bottom face only (BB). Both beams demonstrate a linear relationship between load and displacement during the initial loading phase, reflecting elastic behavior. The retrofitted beam (BB) appears to have a slightly lower initial stiffness compared to the control beam, as indicated by the more gradual slope of the curve in the elastic region. As the load increases, both beams exhibit nonlinear behavior, which corresponds to the initiation of cracking and other inelastic deformations. The retrofitted beam (BB) starts showing signs of nonlinearity at a slightly higher load than the control beam, indicating that the BFRP fabric on the bottom face effectively enhances the beam's resistance to cracking and initial damage.

5 Conclusion

Enhanced Load-Carrying Capacity:

1. The retrofitted beams exhibited a marked improvement in load-carrying capacity compared to the control beam (CB). The BU configuration demonstrated the most significant enhancement, achieving a 17.7% increase in load capacity over the control beam, with an average failure load of 120.30 kN compared to the control beam's 102.72 kN.

2. The BB configuration also showed a substantial increase, with an average failure load of 105.58 kN, resulting in a 2.79% improvement over the control beam. The BS configuration, while less impactful, still provided benefits in load capacity.

Improved Deflection and Ductility:

1. The deflection capacity at failure was significantly improved in the retrofitted beams. For instance, the BB configuration allowed the beam to reach a deflection of 6.449 mm at failure, indicating improved ductility compared to the control beam.

2. The BU configuration also showed enhanced ductility, with deflections up to 7.015 mm, allowing the beam to sustain higher loads with increased deformation before failure.

Ductile Failure Behavior:

The load-deflection curves indicated that the retrofitted beams, especially those in the BU and BB configurations, experienced a more controlled and ductile failure compared to the control beam. The gradual decline in load after reaching peak capacity suggests that BFRP retrofitting enhances the beam's ability to absorb energy and resist collapse, which is critical in structural applications.

Strategic Retrofitting Effectiveness:

The study confirms that the strategic placement of BFRP fabric, particularly on the bottom face of RC beams, significantly enhances structural performance. The BB and BU configurations provided the best combination of increased load capacity and improved ductility, making these configurations particularly effective for retrofitting purposes.

Future Research Directions:

Further studies should investigate the long-term performance of BFRP-retrofitted beams under environmental and cyclic loading conditions. Additionally, exploring different fiber orientations and the use of hybrid materials could further optimize retrofitting strategies.

REFERANCE

ACI Committee 440 (2015). Guide for the Design and Construction of Structural Concrete Reinforced with Fiber-Reinforced Polymer (FRP) Bars (ACI 440.1R-15). American Concrete Institute, Farmington Hills, MI.

ANSYS Inc. (2023). ANSYS Mechanical APDL Documentation. [Online] Available: https://www.ansys.com/products/structures/ansys-mechanical

Bischoff, P. H., & Perry, S. H. (1991). "Compressive behaviour of concrete at high strain rates." Materials and Structures, 24, 425-450.

Chajes, M. J., Finch, W. W., Januszka, T. F., & Thomson, T. A. (1996). "Bond and Force Transfer of Composite Material Plates Bonded to Concrete." ACI Structural Journal, 93(2), 208-217.

Chen, J. F., & Teng, J. G. (2003). "Shear capacity of FRP-strengthened RC beams: FRP debonding." Construction and Building Materials, 17(1), 27-41.

GangaRao, H. V. S., & Vijay, P. V. (1998). "Bending Behavior of Concrete Beams Wrapped with Carbon Fabric." Journal of Structural Engineering, 124(1), 3-10.

IS 456:2000 (2000). Indian Standard Plain and Reinforced Concrete - Code of Practice. Bureau of Indian Standards, New Delhi.

Malek, A. M., & Saadatmanesh, H. (1998). "Analytical Study of Reinforced Concrete Beams Strengthened with FRP Plates." Journal of Structural Engineering, 124(9), 1039-1052.

Nanni, A., & Bradford, N. M. (1995). "FRP jacketed concrete under uniaxial compression." Construction and Building Materials, 9(2), 115-124.

Park, R., & Paulay, T. (1975). Reinforced Concrete Structures. John Wiley & Sons, New York.

Teng, J. G., Chen, J. F., Smith, S. T., & Lam, L. (2002). FRP-Strengthened RC Structures. John Wiley & Sons, West Sussex, England.

Triantafillou, T. C., & Plevris, N. (1992). "Strengthening of RC beams with epoxy-bonded fibre-composite materials." Materials and Structures, 25(4), 201-211.

Xiong, G., Wu, Z., & Liu, H. (2007). "Experimental study on the flexural behavior of reinforced concrete beams strengthened with near-surface mounted CFRP strips." Journal of Composites for Construction, 11(4), 383-389.

Zhang, Z. & Hsu, C. T. T. (2005). "Shear Strengthening of Reinforced Concrete Beams Using Carbon-Fiber-Reinforced Polymer Laminates." Journal of Composites for Construction, 9(2), 158-169.

Zhou, Y., & Teng, J. G. (2006). "Shear behavior of FRP-strengthened RC beams: Assessment of existing models." Journal of Composites for Construction, 10(4), 291-303.